January, 1993] © *1993 The Chemical Society of Japan* *Bull. Chem. Soc. Jpn.,* ***66****, 51—56(1993)* 51

Pressure Dependence of the Rate Constant for the Reaction of CH_3O + NO

Kenji OHMORI,[†] Katsuyoshi YAMASAKI, [††] and Hiroyuki MATSUI*
Department of Reaction Chemistry, Faculty of Engineering, The University of Tokyo, 7-3-1, Hongo, Bunkyo-ku, Tokyo 113

(Received August 6, 1992)

The reaction of CH_3O with NO was examined at room temperature ($T=296\pm6$ K), where, CH_3O was produced in 266 and 355 nm photolysis of CH_3ONO, and detected by laser-induced fluorescence technique. From the time resolved analysis of CH_3O with excess amount of NO, the rate constant for reaction $CH_3O+NO(+M)\rightarrow$ products (+M) (1) was measured over the total pressure range of 7—100 Torr[He], 10—70 Torr[N_2], 15—50 Torr[CF_4], and 10—50 Torr[SF_6] (1 Torr=133.322 Pa). The high-pressure limiting rate constant for reaction (1) has been evaluated to be $k_{1\infty}=(4.5\pm1.5)\times10^{-11}$ cm^3 molecule^{-1} s^{-1} with Hinshellwood-Lindemann theory. The present result is found to be consistent with that obtained recently by Frost and Smith.

Alkoxyl radicals (RO) are known to be important reaction intermediates both in the oxidation of hydrocarbons in combustion processes and the atmospheric chemistry.

There have been numerous studies on the mechanism for production and consumption of these radicals. They are mainly formed in the decomposition of dialkyl peroxides ($ROOR'\rightarrow RO+RO'$) in low temperature combustion, or the reactions of alkyl dioxyl radicals with nitric oxide or atomic oxygen ($ROO+NO/O\rightarrow RO+NO_2/O_2$) in photochemical smog formation cycles. Subsequently, they undergo a variety of reactions and generally produce aldehydes, ketones, and alcohols in these reaction systems.[1,2)]

The reaction of CH_3O, the simplest alkoxyl radical, with NO

$$\begin{array}{lll} CH_3O+NO & \rightarrow CH_3ONO & \text{(Ia)} \\ & \rightarrow CH_2O+HNO & \text{(Ib)} \end{array}$$

has been studied by several groups: Arden et al.[3)] examined the pyrolysis of $(CH_3O)_2$ at 447 K and deduced that $k_{1b}/k_1=0.33$. Wiebe et al.[4)] photolyzed CH_3ONO at 298±2 K, and analyzed products by gas chromatography after 0—220 min irradiation. From the yields of N_2O and N_2, they predicted that $k_{1b}/k_1=0.145$. The rate of decomposition of CH_3ONO was studied by Batt et al.[5)] in the presence of NO (0.9—1.0 atm) at 443—473 K. By using thermochemical data for CH_3O, NO, and CH_3ONO, k_{1a} was estimated to be $10^{-13.7\pm0.2}$ cm^3 molecule^{-1} s^{-1}, assuming that the activation energy for reaction (Ia) is zero.

Subsequently, CH_3O was proved by laser induced fluorescence technique (LIF) with sufficiently high sensitivity.[6)] Although direct examination of the reaction mechanism on CH_3O has become possible without being disturbed by the side reactions owing to this improvement, there have been only limited numbers of such studies so far.

The first direct measurement on kinetic processes of CH_3O radical via LIF technique was conducted by Sanders et al.[7)] They decided the rate constant for reaction (I), k_1 to be $(2.08\pm0.12)\times10^{-11}$ cm^3 molecule^{-1} s^{-1} at 15±5 Torr (1 Torr=133.322 Pa) for SF_6 as a chaperon. They also mentioned that k_1 is in the fall-off region at this pressure range, but no systematic examination of the pressure dependence was presented.[8)]

Recently, two groups examined the pressure dependence of k_1 at a wider pressure range using the same detection technique as Sanders et al.

Zellner[9)] reported that k_1 was slightly dependent on the total presssure, where they used He as a buffer gas, i.e., $k_1=6\times10^{-12}$ cm^3 molecule^{-1} s^{-1} at 4 Torr and increased to $k_1=11\times10^{-12}$ cm^3 molecule^{-1} s^{-1} at 200 Torr. He deduced the high-pressure limiting rate constant for reaction (I); $k_{1\infty}=1.4\times10^{-11}$ cm^3 molecule^{-1} s^{-1} from the extrapolation of the observed fall-off curve using RRK analysis.

Frost and Smith[10)] also examined the pressure dependence of k_1 over a total pressure range of 3—125 Torr at four temperatures between 296 and 573 K using Ar and CF_4 as bath gases. They estimated $k_{1\infty}$ with extended Lindeman theory, which takes into account the two competing pathways (Ia) and (Ib). The rate constant was expressed by $k_{1\infty}=3.6(T/298)^{-0.6}$ cm^3 molecule^{-1} s^{-1}, which leads to $k_{1\infty}=3.6\times10^{-11}$ cm^3 molecule^{-1} s^{-1} at 296 K.

There remains substantial discrepancy on the estimated high-pressure limiting rate constants among these studies. Such discrepancy was not due to the methods for analyses of estimating high-pressure limiting rate constant, but apparently caused by the inconsistency of the measured rate constants for Reaction (I) at the fall-off region. Thus, reinvestigation for this reaction process seems to be important (for example, in estimating life time of CH_3O radicals in the photochemical smog cycle).

In this study, the pressure dependence of k_1 was investigated in the pressure fall-off region for He, N_2, CF_4, and SF_6 as buffer gases to make a detailed examination of the fall-off behavior of the rate constant and to estimate the high-pressure limiting rate constant for the

---

[†] Present address: Research Institute for Scientific Measurements, Tohoku University.

[††] Present address: Department of Chemistry, Niigata University.

titled reaction.

Experimental System

All the experimental informations were obtained by means of a laser photolysis/LIF system in a quasistatic reaction cell.

The reaction cell was made of a Pylex glass with a 35 cm long main tube with a 15 cm short arm perpendicular to each other. A port for a photomultiplier grazing was attached at the crossing point of the two arms. The edges of those two arms and the PMT port were sealed with quartz windows. CH_3ONO, NO, and the buffer gas were mixed before they were injected into the reactor.

The third harmonic (355 nm) or the fourth harmonic (266 nm) of an Nd:YAG laser (Quanta-Ray, DCR-2) was used to photolyze CH_3ONO without focusing. The photolysis laser beam was fed into the main tube along its axis and was parallel to the gas flow. Photolysis energy was about 4 mJ per pulse for both cases and the repetition rate was varied from 4.9 to 7 Hz according to the flow velocity of each buffer gas.

The excitation wave length 355 nm corresponds to the $v'=2$ of $N=0$ stretching progression of the first electronically excited state of CH_3ONO.[11] In this case, CH_3O is produced via a predissociation of CH_3ONO. On the other hand, 266 nm is located in the second electronically excited state, which is broad in the UV absorption spectra of CH_3ONO[11] and is expected to be a repulsive state. Although the mechanism of the photodissociation is different in these two cases, no difference for the measured rate constant was observed. Although the quantum yields for the production of $CH_3O(\Phi_{CH_3O})$ via 266 and 355 nm photolysis of CH_3ONO have not been exactly decided yet, the initial concentration of CH_3O in this study was estimated to be in the range of $(0.1—1)\times10^{12}$ molecule cm^{-3} by assuming $\Phi_{CH_3O}=1$.

CH_3O was probed by using a laser induced fluorescence method (LIF) with a XeCl excimer laser (Lambda Physik, LPX110i) pumped dye laser (PRA, DL14P) operating with Rhodamin 6G. The output of the dye laser was frequency-doubled with a KDP doubling crystal (INRAD, R6G) and tuned to the $\nu_3:4 \leftarrow 0$ band (292.7 nm) of the $\tilde{X}^2E$-$\tilde{A}^2A_1$ transition of CH_3O.[6] A fundamental visible laser beam was blocked with a UV filter (Toshiba, UV-D33S). The UV beam was passed into the short arm normal to the photolysis laser beam and gas flow.

The intensity of the dye laser beam was monitored behind the reaction cell, by reflecting a small fraction of it with quartz disks onto a photodiode (Hamamatsu, S1722-02).

The fluorescence was collected onto a photomultiplier (Hamamatsu Photonics, R-1463-01) with a UV filter (Toshiba, D-36C) in front of it. The output of the photomultiplier was fed into a gated boxcar integrator (Stanford Research Systems, SR250) and then stored in a microcomputer. The Q-switch sync. out pulse of a Nd:YAG laser was used to trigger the boxcar integrator and the XeCl excimer laser. The delay time between the photolysis pulse and probe pulse was scanned with an automatic gate scanner (Stanford Research, SR 200).

The flow rates of the sample gases were measured with a calibrated capacitance manometer (MKS 122AA-00100ab), and concentrations of each component was calculated from the flow rates and their partial pressures. Typical partial pressure of CH_3ONO was 1 mTorr.

Sample gases were: He (Nippon Sanso, 99.9999%), CF_4 (Takachiho Kagaku Kogyo, 99.999%), SF_6 (Kanto Denka, 99.999%), N_2 (Nippon Sanso, 99.9999%), NO (Nippon Sanso, 99.9%), and 2.021% NO/He mixture (Sumitomo Seika) used without further purification. Methyl nitrite was prepared by dropwise addition of H_2SO_4 (one part of acid to two of water) to a mixture of CH_3OH and $NaNO_2$ in molecular proportions, diluted with the same volume of water, under an atmosphere of He.[12] The products were carried over by a helium flow and condensed at 77 K. The reaction products were degassed at 113 and 193 K and distilled by 193 K to 77 K and 163 K to 143 K trap to trap distillation. CH_3ONO was finally collected at 143 K as a pale yellow liquid and stored at 193 K at a dark place. The purity of the final product was confirmed by observing UV absorption spectra at around 320, 339, and 364 nm.

All the experiments were performed at room temperature ($T=296\pm6$ K). The pressure ranges of the buffer gases were; 7—100 Torr[He], 10—70 Torr[N_2], 15—50 Torr[CF_4], 10—50 Torr[SF_6]. All the indicated error limits represent 2 standard deviations.

Experimental Results

Experiment of this study was performed with the presence of excess NO ($[NO]_0>200[CH_3O]_0$ where subscript 0 denotes $t=0$).

Fluorescence intensity of CH_3O showed single-exponential decay profiles with the reaction time. A series of such profiles with different NO concentrations are shown in Fig. 1, where SF_6 was used as a buffer gas.

Logarithmic least-squares fits of these profiles gave pseudo-first-order rates. These first-order decay rates of CH_3O fluorescence intensity were linearly dependent on the concentration of NO as shown in Fig. 2. From the slopes of such plots, overall bimolecular rate constants for reaction (I), k_1, were obtained for each buffer gas at various total pressures.

The total pressure dependencies of k_1 for four different buffer gases (He, N_2, CF_4, and SF_6) are summarized in Table 1: It was found that k_1 was in the fall-off region in all cases under the present experimental conditions.

It was also confirmed that, at a fixed total pressure, the rate constant increased as the number of the vibrational modes of the buffer gas increased (except that it appeared no significant difference between He and N_2). This may indicate the size effect of the collision partner in stabilizing energized CH_3ONO produced via a recombination of CH_3O and NO.

Discussion

Although it has not yet been determined experimentally whether reaction (Ib) is a direct abstraction, or an addition-elimination processes, ab initio calculation performed by McKee[13] indicates the barrier height for addition-elimination pathway is only 2.6 kcal mol^{-1}, so the latter pathway seems favorable at room tempera-

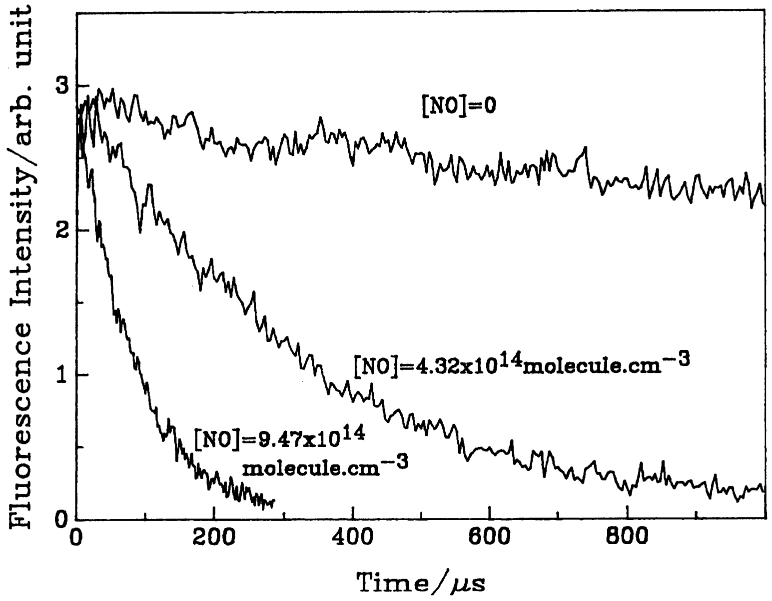

Fig. 1. Decay profiles of LIF intensity of CH_3O. [1 mTorr CH_3ONO+15.3 Torr SF_6, T=297.9 K].

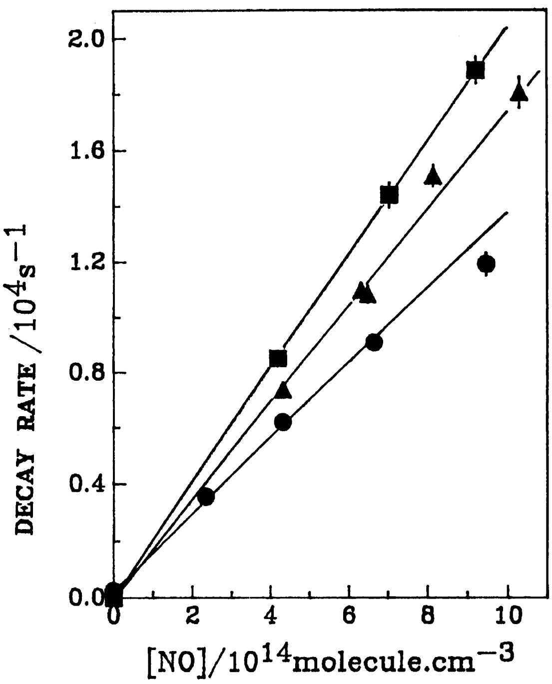

Fig. 2. Pseudo-first-order dependence of the decay rates of CH_3O vs. added NO diluted in SF_6. [total pressure; ●: 15.3 Torr, ▲: 40.5 Torr, ■: 50.6 Torr, T=297.0±1.8 K].

ture, rather than the former which is expected to have much higher barrier for the transition state. Accordingly, reaction (Ib) is assumed as an addition-eliminaiton pathway in the following discussion. In this case, the reaction scheme is described as follows:

$$CH_3O + NO \underset{k_{-r}}{\overset{k_r}{\rightleftarrows}} CH_3ONO\cdot \xrightarrow{k_q[M]} CH_3ONO \quad (1a)$$

$$\xrightarrow{k_d} CH_2O + HNO \quad (1b)$$

Table 1. Summary of the Observed Rate Constant k_1 for the Reaction $CH_3O+NO\rightarrow$ Products, Measured in This Study

Buffer gas	Total pressure	$10^{11}\times k_1$
	Torr	cm^3 $molecule^{-1}$ s^{-1}
He	6.5	0.79±0.02
	14.8	1.00±0.05
	15.0	0.96±0.03
	23.7	1.11±0.08
	35.2	1.31±0.15
	50.1	1.38±0.07
	69.3	1.63±0.17
	83.2	1.74±0.12
	101.3	2.11±0.13
N_2	11.2	0.99±0.02
	15.1	1.16±0.06
	25.1	1.19±0.10
	40.3	1.28±0.19
	56.0	1.38±0.10
	70.4	1.49±0.16
CF_4	15.0	1.14±0.02
	30.0	1.33±0.06
	40.0	1.42±0.16
	50.0	1.71±0.09
SF_6	10.0	1.34±0.04
	15.3	1.35±0.07
	15.3	1.34±0.03
	30.2	1.62±0.12
	40.5	1.74±0.06
	50.1	2.14±0.14
	50.6	2.04±0.01

The high-pressure limiting rate constant for reaction (1), $k_{1\infty}$ was estimated in this study using Hinshelwood-Lindemann theory, as was tried by Frost and Smith.[10] In this analysis, the following useful relationship is derived:

$$k_1/(1-k_1/k_{1\infty}) = k_{bo} + k_{ao}[M] \quad (2)$$

where, $k_{ao}=(k_r/k_{-r})k_q$, $k_{bo}=(k_r/k_{-r})k_d$, k_1 is the observed overall bimolecular rate constant for reaction (1) at the pressure fall-off region, and $k_{1\infty}$ is the high-pressure limiting rate constant for reaction (1). Namely, the left-hand side of this equation is linearly dependent on the total pressure. The best fits to the experimental data were searched for with use of Eq. 2. An example of the analyses is shown in Fig. 3. Since $k_{1\infty}$ and k_{bo} should be unchanged with variation of a buffer gas, a common k_{bo} for different buffer gases were repeatedly searched for against different values of assumed $k_{1\infty}$.

Common $k_{1\infty}$ and k_{bo} for the series of the buffer gases could be obtained when $k_{1\infty}$ was assumed to be less than 6×10^{-11} cm^3 molecule^{-1} s^{-1}, where, the uncertainties of the measured rate constants k_1 (standard deviation of 2σ) were taken into account.

Uncertainties for k_{bo} increased very rapidly when $k_{1\infty}$ was less than 3×10^{-11} cm^3 molecule^{-1} s^{-1}, although the calculated k_{bo} were still overlapping each other for different collision partners. Also, the standard deviations for the values of k_{ao} became too large as $k_{1\infty}$ was reduced. This indicates that the linear correlation given by Eq. 2 is not optimized in this range.

At higher range of $k_{1\infty}$ ($>6\times10^{-11}$ cm^3 molecule^{-1} s^{-1}), the linear correlations of Eq. 2 still hold with good accuracies for all the buffer gases, but apparently, a common value for k_{bo} could not be found even if experimental uncertainties were taken into account.

As a consequence, it was concluded that the best consistency was attained for $k_{1\infty}=(4.5\pm1.5)\times10^{-11}$ cm^3 molecule^{-1} s^{-1}, and the averaged value for k_{bo} (weighted for the numbers of the data point) was $(10.2\pm3.0)\times10^{-12}$ cm^3 molecule^{-1} s^{-1}. The low-pressure limiting rate constants for reactions (1a) and (1b), i.e. k_{ao} and k_{bo} decided in this study for each buffer gas are summarized in Table 2, compared with those by Frost and Smith:[10] k_{ao} evaluated in this study for CF$_4$ as a chaperon was found to be about half of that evaluated by Frost and Smith for the same buffer gas.

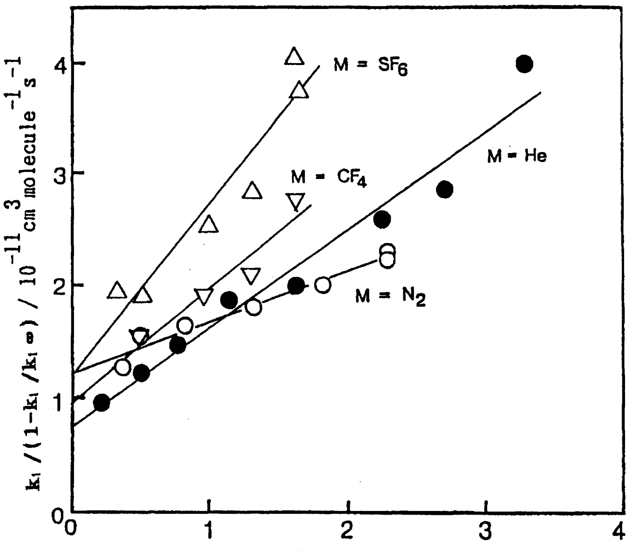

Fig. 3. Plots of $k_1/(1-k_1/k_{1\infty})$ vs. total pressure for various buffer gases. [●: M=He, ○: M=N$_2$, ▽: M=CF$_4$, △: M=SF$_6$, the straight lines denote the least-squares fit of the experimental data, $k_{1\infty}=4.5\times10^{-11}$ cm^3 molecule^{-1} s^{-1}].

Previous direct measurements of the rate constant for reaction (1)[7,9,10] are compared with those of this study in Fig. 4. All the measured rate constants are in the pressure fall-off region.

The pressure dependencies of k_1 measured in this study and measured by Frost and Smith[10] for CF$_4$ as a bath gas are consistent with each other. The discrepancy between k_1 measured in this study and those by Zellner[9] for He as a bath gas becomes larger as the total pressure increases. It is not clear why such a disagreement between these two studies was introduced.

Table 2. Comparison of the Present and Previous Low-Pressure Limiting Rate Constants for Pathways (1a) and (1b) at Room Temperature[a)]

Buffer gas	k_{ao}[b)]	k_{bo}[c)]	Reference
He	0.86±0.13	0.77±0.23	This work
N$_2$	0.43±0.10	1.24±0.10	This work
CF$_4$	1.01±0.45	0.95±0.53	This work
SF$_6$	1.55±0.40	1.18±0.44	This work
Ar	1.50	0.55	10
CF$_4$	1.85	0.55	10

a) k_{ao} and k_{bo} are estimated for $k_{1\infty}=4.5\times10^{-11}$ cm^3 molecule^{-1} s^{-1}. b) The low-pressure limiting rate constant for reaction (1a) (units in 10^{-29} cm^6 molecule^{-2} s^{-1}). c) The low pressure-limiting rate constant for reaction (1b) (units in 10^{-11} cm^3 molecule^{-1} s^{-1}).

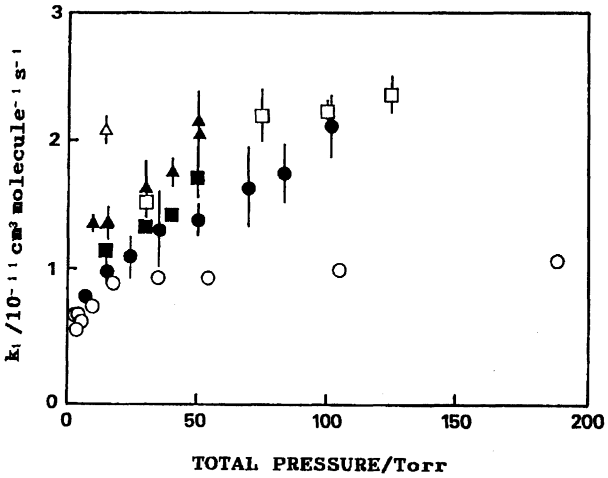

Fig. 4. Summary of the experimental results on the rate constants for reaction (1) at room temperature. [△: Sanders et al.[7] (M=SF$_6$), ○; Zellner[9] (M=He), □; Frost and Smith[10] (M=CF$_4$), ●; this study (M=He), ■; this study (M=CF$_4$), ▲: this study (M=SF$_6$)].

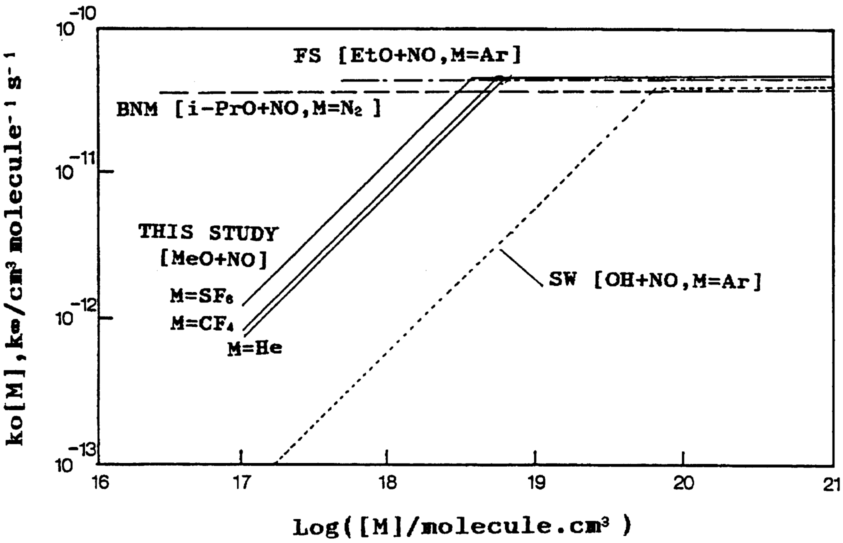

Fig. 6. Comparison of the transition concentration from the low-pressure limiting rate k_0[M] to high-pressure limiting rate constant k_∞ for the reactions of OH and alkoxyl radicals with NO. [FS: Frost and Smith,[10] BNM: Balla et al.,[18] SW: Smith and Williams[19]].

Sanders et al. reported briefly that reaction (1) was in the fall-off region at 15±5 Torr [SF_6].[8] Their value for $k_{1\infty}$ should be therefore larger than 2.08×10^{-11} cm^3 molecule^{-1} s^{-1}: This conclusion was consistent with the present result, however, the magnitude of k_1 measured by Sanders et al. was about 1.5 times larger than those measured at the same pressure range of this study with the same buffer gas. The initial concentrations of CH_3O in the experiment by Sanders et al. were estimated to be in the range of $(1—8)\times10^{13}$ molecule cm^{-3} based on the quantum yield for the production of CH_3O at 248 nm.[14] Thus, their experiment was performed with the initial concentrations of CH_3O of about an order of magnitude higher than this study. The difference of the initial concentrations of CH_3O might be responsible for such a discrepancy because of the effects of side reactions on the decay rates of CH_3O.

The high-pressure limiting rate constants for reactions of NO with higher alkoxyl radicals[10,15—18] k_∞ are compared with $k_{1\infty}$ for CH_3O+NO in Fig. 5: The high-pressure limiting rate constants for reactions of alkoxyl radical with NO seems to be insensitive to the size of the radicals, and all the rate constants for RO+NO seem to be in the range of $(3—6)\times10^{-11}$ cm^3 molecule^{-1} s^{-1} except for Zellner's measurements.

According to the RRKM theory,[20] magnitude of k_∞ is proportional to Q^*/Q, i.e., the ratio of the partition functions for the transition state and the reactants. Although magnitudes of the partition functions have large dependence on molecular size, Fig. 5 indicates that the imaginary vibrational frequency nor barrier height of the transition structure for the association of RO+NO channel (and other factors that contribute to the ratio Q^*/Q) are not changed so much by increasing the size of alkoxyl radical.

In contrast, the transition pressure for reaction of RO radical (R=H or alkyl radical) with NO is found to have a correlation with the size of R. In Fig. 6, the fall-off behavior of the bimolecular rate constants for OH+NO,[19] CH_3O+NO (this study), C_2H_5O+NO,[10] and i-C_3H_7O+NO[18] is described by using k_0 [M] and k_∞, where M is the third body and k_0 and k_∞ are the low-pressure and high-pressure limiting rate constants, respectively. The transition pressure $p_{1/2}$ is reduced as R becomes complex.

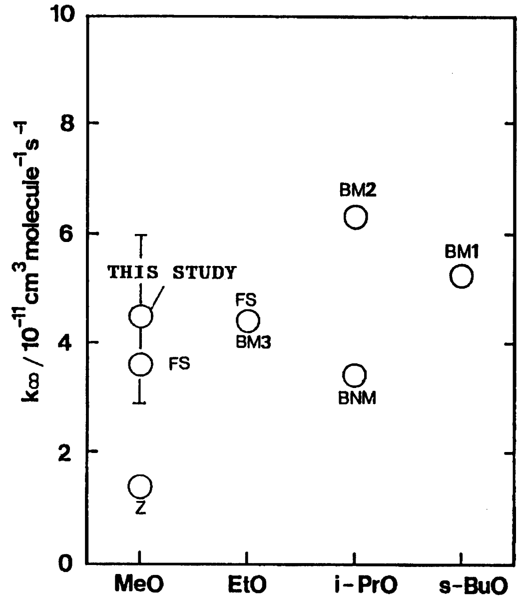

Fig. 5. Summary of the measured high-pressure limiting rate constants for the reaction of alkoxyl radicals with NO. [Z: Zellner,[9] FS: Frost and Smith,[10] BM1: Batt and McCulloch,[15] BM2: Batt and Milne,[16] BM3: Batt and Milne,[17] BNM: Balla et al.[18]].

This implies that the rate of intramolecular energy transfer in energized RONO, k_e becomes fast as the molecular size of the alkoxyl radical increasese, because the transition pressure $p_{1/2}$ is expressed as

$$p_{1/2} = k_\infty / k_e \tag{3}$$

by the simple Lindemann theory.

Finally, it should be pointed out that the process (1b) was estimated as minor in reaction (1) but had substantial contribution (specially at low pressure range) as is shown in Table 1. Although the present result on k_{bo} was consistent with that by Frost and Smith,[10] the analysis in these studies was based on the extended Lindemann theory which seems too simple to extract such infomation; so the estimated k_{bo} may have large uncertainty. It is desirable to decide the branching ratio for reaction (1) directly.

Measurement of the branching fractions for reaction (1) was tried in this study by using a microwave-discharge flow reactor equipped with a LIF system and an electron impact mass spectrometer for sensing CH_3O and CH_3ONO, respectively. CH_3O was prepared in this case by using the reaction, $CH_3OH+F \rightarrow CH_3O+HF$, where, F atoms were produced by microwave-descharge of F_2. However, the rate of heterogeneous reaction at the tube wall was relatively large, and also stability of the mass signal for CH_3ONO was not sufficient enough to decide the branching fractions accurately. Further challenge to the examination of reaction mechanism of (1) seems still meaningful.

Valuable discussions with Professors M.C. Lin of Emory University, and Mitsuo Koshi of The University of Tokyo are gratefully acknowledged. This work was partly supported by Grant-in-Aid for Scientific Research on Priority Areas "Exploration of Combustion Mechanism" of the Ministry of Education, Science, and Culture (Contract No. 01627504).

References

1) R. T. Pollard, in "Comprehensive Chemical Kinetics," ed by C. H. Bamford and C. F. H. Tipper, Elsevier, New York (1977), Vol. 17, Chap. 2.

2) J. N. Bradley, "Flame and Combustion Phenomena," Methuen, London (1969).

3) E. A. Arden, L. Phillips, and R. Shaw, *J. Chem. Soc.*, **1964**, 5126.

4) H. A. Wiebe and J. Heicklen, *J. Am. Chem. Soc.*, **95**, 1(1973).

5) L. Batt, R. T. Milne, and R. D. McCulloch, *Int. J. Chem. Kinet.*, **9**, 567(1977).

6) G. Inoue, H. Akimoto, and M. Okuda, *J. Chem. Phys.*, **72**, 1769(1980).

7) N. Sanders, J. E. Butler, L. R. Pasternack, and J. R. McDonald, *Chem. Phys.*, **48**, 203(1980).

8) D. Gutman, N. Sanders, and J. E. Butler, *J. Phys. Chem.*, **86**, 66(1982).

9) R. Zellner, *J. Chim. Phys.*, **84**, 403(1987).

10) M. J. Frost and I. W. M. Smith, *J. Chem. Soc., Faraday Trans.*, **86**, 1757(1990).

11) J. G. Calvert and J. N. Pitts, Jr., "Photochemistry," John Wiley and Sons, New York (1966).

12) W. K. Slater, *J. Chem. Soc.*, **117**, 587(1920).

13) M. L. Mckee, *J. Am. Chem. Soc.*, **108**, 5784(1981).

14) F. Ewig, D. Rhasa, and R. Zellner, *Ber. Bunsen-Ges. Phys. Chem.*, **91**, 708(1987).

15) L. Batt and R. D. McCulloch, *Int. J. Chem. Kinet.*, **8**, 911(1976).

16) L. Batt and R. T. Milne, *Int. J. Chem. Kinet.*, **9**, 141(1977).

17) L. Batt and R. T. Milne, *Int. J. Chem. Kinet.*, **9**, 549(1977).

18) R. J. Balla, H. H. Nelson, and J. R. McDonald, *Chem. Phys.*, **99**, 323(1985).

19) I. W. M. Smith and M. D. Williams, *J. Chem. Soc., Faraday Trans. 2*, **91**, 4653(1987).

20) P. J. Robinson and K. A. Holbrook, "Unimolecular Reactions," John Wiley and Sons, New York (1972).